Numerical investigation of DDT process in a channel with grooves

Hiroaki Shiga[1], Edyta Dzieminska[1], Wu Bing[1], Nobuyuki Tsuboi[2]
[1]Sophia University, Tokyo, Japan
[2]Kyushu Institute of Technology, Kitakyushu, Japan

1 Introduction

In recent years, hydrogen fuel—which emits no carbon dioxide during combustion—has attracted significant attention as global warming intensifies. The International Energy Agency (IEA) has emphasized the importance of hydrogen utilization, along with improved energy efficiency and increased use of renewable energy, in its roadmap to achieve net-zero CO_2 emissions by 2050 [1]. However, hydrogen presents significant safety challenges, particularly due to its high flammability when mixed with oxidizers. Accidents have frequently been reported in transportation pipelines and storage facilities [2]. When hydrogen and an oxidizer ignite within a pipeline, a detonation—defined as a supersonic combustion wave accompanied by shockwaves—can occur. Such events may cause severe structural damage and pose serious safety risks. As a result, considerable research has focused on hydrogen detonation from a safety engineering perspective.

This study aims to investigate the mechanisms of hydrogen detonation initiation and propagation, with a particular focus on grooved combustion channels—a configuration that has received limited attention in prior research. Additionally, it examines how such grooves influence the onset of detonation.

2 Numerical setups

2.1 Governing equations

Because detonation propagates at approximately 4 to 6 times the speed of sound, the influence of molecular diffusion and boundary-layer viscosity on the detonation wave is generally negligible. For this reason, the Euler equations are commonly used in numerical analyses of detonation phenomena. However, to investigate the deflagration-to-detonation transition (DDT) in this study, we employ the two-dimensional compressible Navier-Stokes equations, which account for viscosity, mass diffusion, and heat conduction resulting from chemical reactions.

The governing equations are derived from the conservation laws of mass, momentum, energy, and individual chemical species in compressible reactive fluid dynamics. When extended to a two-

Correspondence to: edyta.d@sophia.ac.jp

dimensional Cartesian coordinate system, the Navier-Stokes equations incorporating mass diffusion, viscosity, and heat conduction take the following form:

$$\frac{\partial \boldsymbol{Q}}{\partial t}+\frac{\partial \boldsymbol{E}}{\partial x}+\frac{\partial \boldsymbol{F}}{\partial y}=\frac{\partial \boldsymbol{E}_v}{\partial x}+\frac{\partial \boldsymbol{F}_v}{\partial y}+\boldsymbol{S} \tag{2.1}$$

$$\boldsymbol{Q}=[\rho\ \rho u\ \rho v\ e\ \rho_1\ \ldots\ \rho_N]^T \tag{2.2}$$

$$\boldsymbol{E}=[\rho u\ \ \rho u^2\ \rho v u\ \ (e+p)u\ \ \ \rho_1 u\ \ldots\ \rho_N u\ ]^T \tag{2.3}$$

$$\boldsymbol{F}=[\rho v\ \ \rho u v\ \rho v^2\ \ (e+p)v\ \ \ \rho_1 v\ \ldots\ \rho_N v\ ]^T \tag{2.4}$$

$$\boldsymbol{E}_v=\left[0\ \ \tau_{xx}\ \ \tau_{xy}\ \ \left(\tau_{xx}u+\tau_{xy}v+q_x\right)\ \ \rho D_1\frac{\partial Y_1}{\partial x}\ \ \ldots\ \rho D_N\ \frac{\partial Y_N}{\partial x}\ \right]^T \tag{2.5}$$

$$\boldsymbol{F}_v=\left[0\ \ \tau_{yx}\ \ \tau_{yy}\ \ \left(\tau_{yx}u+\tau_{yy}v+q_y\right)\ \ \rho D_1\frac{\partial Y_1}{\partial y}\ \ \ldots\ \rho D_N\ \frac{\partial Y_N}{\partial y}\ \right]^T \tag{2.6}$$

$$\boldsymbol{S}=[0\ \ 0\ \ 0\ \ 0\ \ M_1\dot{\omega}\ \ldots\ M_N\dot{\omega}\ ]^T \tag{2.7}$$

In this formulation:

- $\boldsymbol{Q}$ represents the time integration terms (conserved variables).
- $\boldsymbol{E}$ and F represent the convective fluxes in the x- and y- directions, respectively.
- $\boldsymbol{E_v}$ and $\boldsymbol{F_v}$ represent the viscous fluxes in the x- and y-directions, respectively.
- $\boldsymbol{S}$ represents the source term vector, including contributions from chemical reactions.

2.2 Chemical reaction model

This study focuses on hydrogen–air premixed combustion, for which the overall reaction is:

$$2\mathrm{H_2}+\mathrm{O_2}\rightarrow 2\mathrm{H_2O} \tag{2.8}$$

In reality, however, numerous elementary reactions occur, producing intermediate species and eventually leading the system to thermal equilibrium. Unlike the overall reaction model, a detailed reaction mechanism comprising elementary reactions enables more accurate analysis of chemically driven transition phenomena. Therefore, the UT-JAXA model developed by Shimizu et al. [3] is employed in this study. This model includes 9 chemical species and 21 elementary reactions, selected through sensitivity analysis to focus on dominant reaction pathways. It achieves a good balance between accuracy and computational efficiency. Furthermore, because CEARUN simulations by NASA indicate that detonation pressure can reach up to 15 times the initial pressure, the UT-JAXA model was selected for its proven validity under high-pressure conditions.

2.3 Grid model, numerical analysis method

The computational grid was generated using Pointwise software and is based on the experimental setup described by Kurup [4]. The mesh consists of 2,793 cells in the x-direction and 143 cells in the y-direction. The average cell size is approximately 0.36 mm × 0.62 mm, although finer mesh resolution is applied in regions with significant geometric variation.

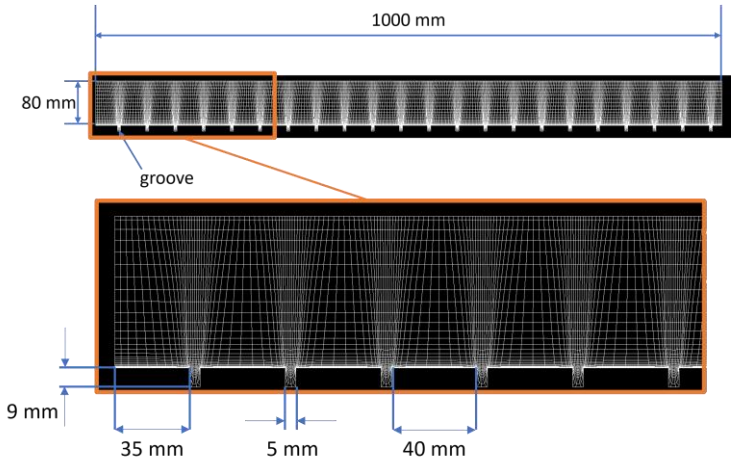

Figure 1: Computational grid.

Temperature, pressure, and density values at each grid point are calculated to track the propagation of combustion waves within the channel. The simulation employs direct numerical simulation (DNS) based on the compressible reactive Navier–Stokes equations described earlier. For convective terms, the HLLC scheme [5] is used, combined with a second-order MUSCL scheme [6] for spatial accuracy, utilizing the minmod limiter. Time integration is performed using the third-order total variation diminishing (TVD) Runge–Kutta method [7], an explicit scheme. Chemical reaction source terms are handled using the point-implicit method.

2.4 Initial conditions

In this study, stoichiometric hydrogen–air premixed gas was used for the numerical analysis. The initial temperature inside the combustion channel was set to 298 K. The initial pressure was varied from 0.2 to 0.7 bar in 0.05 bar increments. To investigate the conditions under which deflagration-to-detonation transition (DDT) occurs, the ignition pressure was varied between 0.50 MPa and 0.70 MPa. The ignition temperature was set to the adiabatic flame temperature corresponding to each ignition pressure.

Table 1: Initial conditions.

	Ambient pressure P_0 [bar]	**Ambient pressure P_0 [atm]**	**Ambient temperature T_0 [K]**	**Ignition pressure P_i [bar]**	**Ignition pressure P_i [atm]**	**Ignition temperature T_i [K]**
(a)	0.45	0.444	298	0.50	4.935	2423
(b)	0.45	0.444	298	0.60	5.922	2428
(c)	0.45	0.444	298	0.70	6.908	2431
(d)	0.20	0.197	298	0.70	6.908	2431
(e)	0.30	0.296	298	0.70	6.908	2431
(f)	0.40	0.395	298	0.70	6.908	2431
(g)	0.50	0.493	298	0.60	5.922	2428
(h)	0.60	0.592	298	0.60	5.922	2428
(i)	0.70	0.691	298	0.60	5.922	2428

3 Results and discussion

The results for an initial pressure of 0.45 bar are presented below.

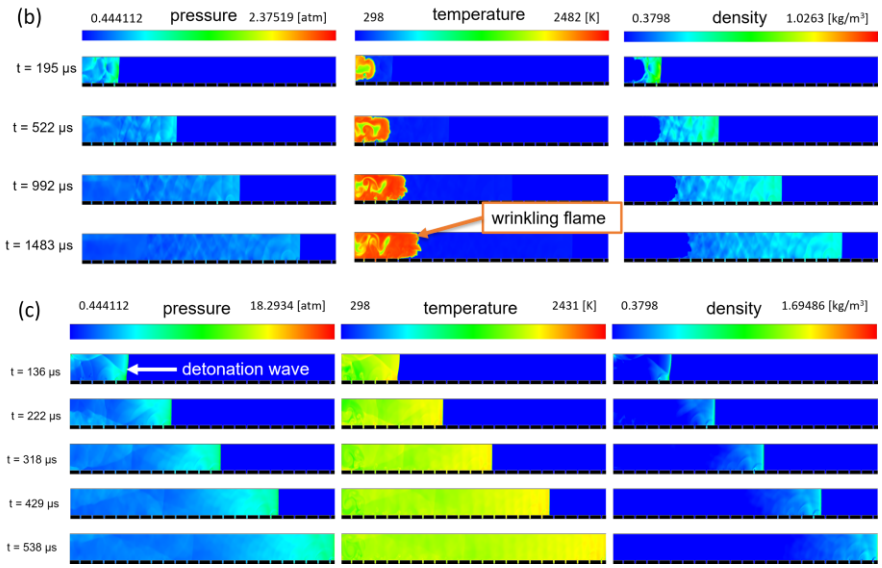

Figure 2: Contour diagrams ((b) and (c)).

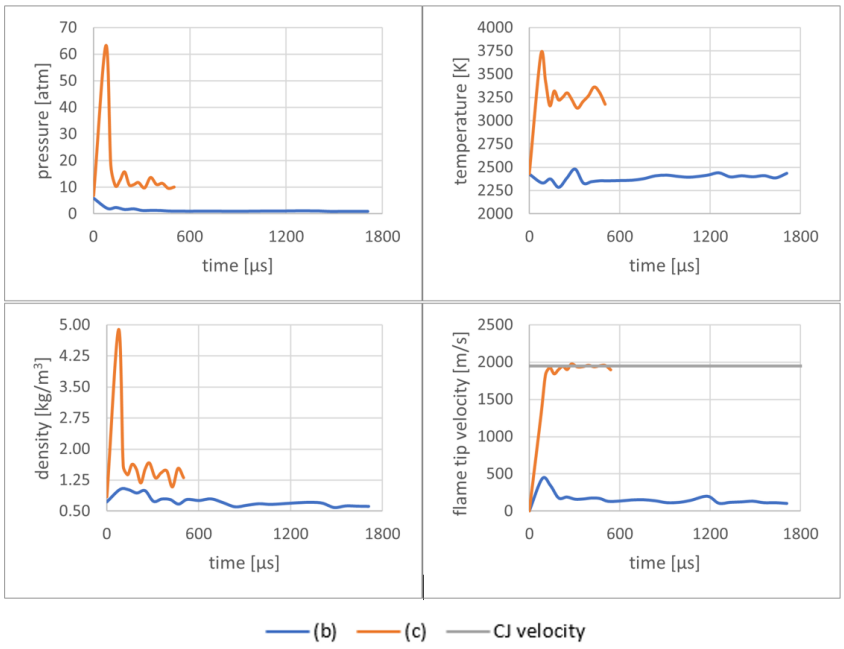

Figure 3: Time dependence of various parameters (maximum value) ((b) and (c)).

As shown in the temperature contour diagram in Figure 2(b), the flame is deformed into a vortex above the groove, with its tip shifting upward due to the reflected wave from the groove. Eventually, the flame becomes increasingly wrinkled due to the induced disturbances, resulting in a larger flame surface area. The density contour indicates that only a compression wave propagates ahead of the flame, and that the flame and the compression wave travel independently. In contrast, Figure 2(c) demonstrates that a shock wave is generated immediately after ignition and propagates in alignment with the flame front.

Furthermore, the temperature contours reveal that the shock wave forms a vortex structure as it passes over the groove.

Figure 3(b) shows the time evolution of the maximum values of various parameters, where oscillations caused by flow disturbances are observed in all quantities. While the flame temperature gradually increases, the pressure and density decrease as the compression wave propagates. Compared to condition (b), the maximum values of pressure, temperature, and density in condition (c) are consistently higher throughout the simulation. As depicted in Figure 3, the flame front velocity under condition (b) increases after ignition but then remains nearly constant, indicating no significant acceleration as the flame evolves. In contrast, under condition (c), the flame front velocity rapidly increases immediately after ignition, reaches the Chapman–Jouguet (CJ) speed at $t = 136\,\mu s$, and subsequently propagates at a nearly constant velocity. Comparing these results with theoretical values obtained from NASA-CEA, it was confirmed that detonation did not occur under condition (b), while successful transition to detonation was observed under condition (c).

Next, we present the results for cases (d) to (i), in which the ignition pressure was fixed while varying the initial pressure.

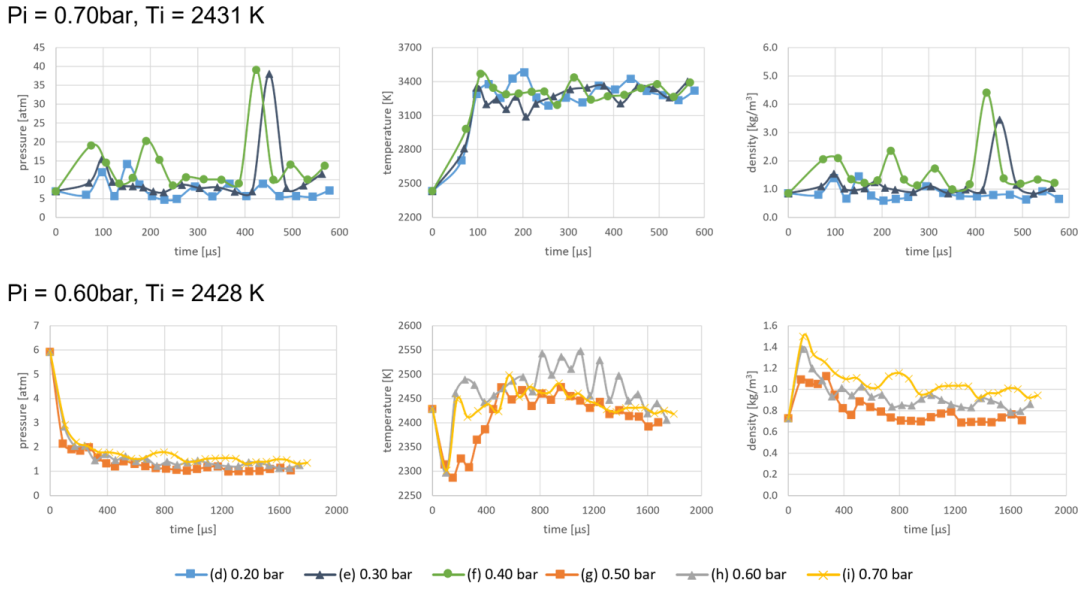

Figure 4: Time dependence of various parameters (maximum value) ((d) to (i)).

In cases (d)–(f), a sudden pressure rise was observed immediately after ignition, indicating the formation of a shock wave. Although the initial fluctuations were smaller than those in case (c), all conditions satisfied the NASA-CEARUN criteria for detonation, confirming the occurrence of detonation via direct ignition (DI). In cases (e) and (f), a secondary increase in pressure was observed at later times; however, this was not accompanied by a corresponding rise in temperature. A near-linear relationship was also observed between the initial pressure and the maximum pressure of the combustion wave, though temperature measurements were affected by disturbances, making precise evaluation difficult.

In contrast, in cases (g)–(i), the pressure dropped sharply in the early stages and eventually stabilized, failing to meet the detonation conditions—similar to case (b). Notably, oscillatory behavior due to flow disturbances was apparent in the time-dependent profile of the maximum temperature, particularly in case (h), where the fluctuations were most significant.

4 Conclusions

This study numerically investigated the flame acceleration and deflagration-to-detonation transition (DDT) behavior of stoichiometric hydrogen–air mixtures in a grooved combustion channel. The results revealed that the presence of grooves induces flame disturbances, leading to increased flame temperature and enhanced formation of wrinkled flame fronts. However, a clear acceleration of the flame due to the grooves was not observed.

A proportional relationship was identified between the initial pressure and key deflagration parameters, such as maximum pressure. Despite varying the initial and ignition pressures, DDT was not observed under any condition. Instead, direct ignition (DI) was the dominant initiation mechanism. This deviation from previous studies may be attributed to insufficient resolution of the shock wave region in the current numerical model.

To improve accuracy, future work should focus on refining the numerical methods, including grid resolution, boundary condition treatment, and chemical reaction modeling. Moreover, since the current analysis was limited to two-dimensional simulations, extending the investigation to three-dimensional domains will be essential to assess whether the observed phenomena persist under more realistic spatial conditions.

During the presentation, the comparison with experimental data will be provided.

Acknowledgments

The calculations in this study were performed using the Large-Scale Computing System (SQUID) at the Cybermedia Center, Osaka University.

References

[1] International Energy Agency, “Net Zero by 2050: A Roadmap for the Global Energy sector,” IEA Publications, France, 2021.

[2] F. Yang, T. Wang, X. Deng, J. Dang, Z. Huang, S. Hu, Y. Li and M. Ouyang, "Review on hydrogen safety issues: Incident," *International Journal of Hydrogen Energy,* vol. 46, no. 61, pp. 31467-31488, 2021.

[3] K. Shimizu, A. Hibi, M. Koshi, Y. Morii and N. Tsuboi, "Update Kinetic Mechanism for High Pressure Hydrogen Combustion," *Journal of Propulsion and Power,* vol. 27, pp. 383-395, 2011.

[4] A. Kurup, “Flame Acceleration and Detonation Initiation in a Grooved Channel,” Sophia University, Chiyoda-ku, Tokyo, 2024.

[5] E. Bernd, “On Godunov-Type Methods for Gas Dynamics,” *SIAM Journal on Numerical Analysis*, 第 巻 25, 第 2, pp. 294-318, 1998.

[6] L. V. Bram, “Towards the ultimate conservative difference scheme. IV. A new approach to numerical convection,” *Journal of Computational Physics*, 第 巻 23, 第 3, pp. 276-299, 1977.

[7] S. Gottlieb , W. C. Shu, “Total Variation Diminishing Runge-Kutta Schemes,” *MATHE MATICS OF COMPUTATION*, 第 巻 67, 第 221, pp. 73-85, 1998.